Chemical Science

EDGE ARTICLE

View Article Online
View Journal | View Issue

Cite this: *Chem. Sci.*, 2016, **7**, 1896

Single near-infrared fluorescent probe with high- and low-sensitivity sites for sensing different concentration ranges of biological thiols with distinct modes of fluorescence signals†

Hua Chen,[b] Yonghe Tang,[a] Mingguang Ren[a] and Weiying Lin*[ab]

We describe a unique approach for the development of an interesting type of the fluorescent probes, which can show different modes of fluorescence signals to distinct concentration ranges of a target of interest. The key points for the design of the new type of the fluorescent probes include the judicious selection of the dye platforms and the corresponding high- and low-sensitivity sites. It is known that the normal concentrations of biological thiols have significant biological functions. However, up- or down-regulated concentrations of thiols may induce several diseases. Therefore, it is highly important to monitor the changes of thiol concentrations in living systems. Based on the proposed strategy, we engineer the novel NIR fluorescent probe, **CHMC-thiol**, which remarkably can display a turn-on signal to the low concentration range of thiols and a ratiometric response to the high concentration range of thiols for the first time. We anticipate that the intriguing strategy formulated herein will be widely useful for the development of concentration range-dependent fluorescent probes.

Received 22nd September 2015
Accepted 24th November 2015

DOI: 10.1039/c5sc03591k

www.rsc.org/chemicalscience

Introduction

Small-molecular-weight biological thiols, including cysteine (Cys), homocysteine (Hcy), and glutathione (GSH), play a critical role in many biological processes. However, abnormal concentrations of Cys, Hcy and GSH are implicated in a variety of diseases, such as liver damage, skin lesions, slowed growth and edema.[1–3] Therefore, it is highly important to monitor the changes of concentrations of thiols in living systems.

Although a large amount of fluorescent probes have been developed,[4–7] among them only a few single fluorescent probes are capable of monitoring multiple targets in living systems with distinct fluorescence signals.[8] A single fluorescent probe with the ability of sensing multiple targets in a consecutive manner imparts several advantages over the combination of several fluorescent probes, as it can avoid the problems such as cross-talk, different localizations, and different metabolisms induced by the combination use of several fluorescent probes. Nevertheless, to the best our knowledge, there is no report yet describing a single fluorescent thiol probe for sensing the different concentration ranges of thiols with distinct fluorescence signals. Thus, it is interesting to develop a probe exhibiting different modes of fluorescence signal for the different concentration ranges of thiols. Obviously, it is very challenging to design such intriguing concentration range-dependent fluorescent probes.

Aware of the great interest for the development of concentration range-dependent fluorescent probes, in particular with near-infrared (NIR) emission properties for potential applications in living animals, several factors should be considered in designing this type of probe. First, the NIR fluorescent dye should have two chemical handles, which can be readily modified to afford two interaction sites for the target of interest. Secondly, the two interaction sites should exhibit distinct sensitivity to the target of interest. This may provide the recognition basis (the interaction step in the overall sensing process). In other words, the probes should contain high and low sensitivity sites for the target of interest. Thirdly, mostly important and challenging, the high-sensitivity site of the probes should interact with the low concentration range of the target to provide one mode of fluorescence signal, while the low-sensitivity site of the probes should interact with the high concentration range of the target to give off the other mode of fluorescence signal. This involves the transduction of the recognition into the optical signal.

In 1992, Patonay *et al.* developed heptamethine cyanine dyes with a rigid chlorocyclohexenyl ring in the methine chain, which is favorable to increase the photostability and

[a]*Institute of Fluorescent Probes for Biological Imaging, School of Chemistry and Chemical Engineering, School of Biological Science and Technology, University of Jinan, Jinan, Shandong 250022, P. R. China*

[b]*State Key Laboratory of Chemo/Biosensing and Chemometrics, College of Chemistry and Chemical Engineering, Hunan University, Changsha, Hunan 410082, China. E-mail: Weiyinglin2013@163.com*

† Electronic supplementary information (ESI) available. See DOI: 10.1039/c5sc03591k

fluorescence quantum yields.[9] The rigid structures also render the chloro group as a reactive site for chemical substitution at the central ring. Recently, our group has presented an approach for the regulation of the fluorescence of merocyanine dyes (**HD** NIR dyes).[10] The dyes are advantageous over the traditional 7-hydroxycoumarin and fluorescein with maximal absorption and emission in the NIR region while retaining an optically tunable hydroxyl group. However, both the traditional chloro-substituted heptamethine cyanine dyes and the recently developed **HD** NIR dyes have only one chemical handle that can be transformed into a reactive site for a target of interest. To address this problem, we envisioned that by the hybridization of the chloro-substituted cyanine and **HD** NIR dye, we may afford an innovative type of NIR dye, **CHMC** (chloro-hydroxyl merocyanine), which, notably, contains a key chloro moiety and a critical hydroxyl group that can be readily transformed into two reactive sites for a target of interest (Fig. 1). We thus anticipated that the novel **CHMC** dye could be exploited as a powerful platform for the design of the concentration range-dependent NIR fluorescent probes for thiols.

After selecting the platform, the next step is to choose the two interaction sites for thiols. With the above design criteria for the innovative fluorescent probes in mind, we proposed the new **CHMC-thiol** (Fig. 2) as a potential candidate probe that may show two modes of fluorescence signals towards low and high concentration ranges of thiols. It is known that the 2,4-dinitrobenzenesulfonate moiety is highly reactive towards thiols,[3g,11] thus, it is reasonable to be selected as the high-sensitivity site for thiols. By contrast, the chloro group is less reactive to thiols, and it was chosen as the low-sensitivity site for thiols.[2c,2f,12] From the optical point of view, the 2,4-dinitrobenzenesulfonate moiety is a notorious fluorescence quencher,[3g,11] thus, we envisioned that interactions of the 2,4-dinitrobenzenesulfonate moiety of the probe **CHMC-thiol** with thiols may provide a turn-on mode in fluorescence. On the other hand, it is known that the nucleophilic substitution of the chloro moiety of chloro-substituted cyanine with heteroatoms (*i.e.* sulfur,[12] nitrogen[9b]) may induce a ratiometric mode in fluorescence. We thus anticipated that, similarly, the nucleophilic substitution of the chloro moiety of the probe **CHMC-thiol** with thiols may induce a ratiometric mode in fluorescence. In this way, the unique

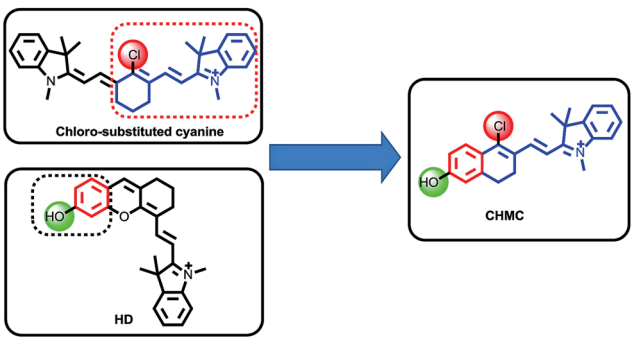

Fig. 1 The design of the novel **CHMC** dye as a representative platform for the concentration range-dependent NIR fluorescent probes by the hybridization of the chloro-substituted cyanine and **HD** NIR dye.

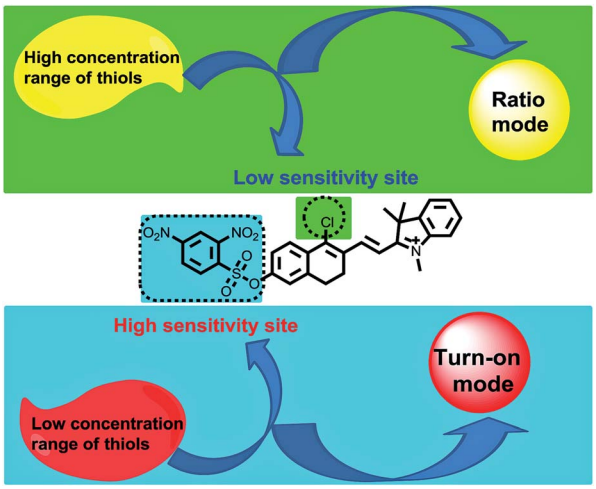

Fig. 2 Rational design of the smart fluorescent thiol probe, **CHMC-thiol** (**CHMC** as a platform for **CHMC-thiol**; the 2,4-dinitrobenzenesulfonate moiety is the high sensitivity site to provide a turn-on mode in fluorescence, and the chloro group is the low-sensitivity site to give off a ratiometric mode in fluorescence).

probe **CHMC-thiol** containing both the high-sensitivity site (the 2,4-dinitrobenzenesulfonate moiety) and the low-sensitivity site (the chloro moiety), may provide a turn-on mode and a ratiometric mode in fluorescence, respectively, upon interactions with thiols.

Results and discussion

Synthesis of the fluorescent probe CHMC-thiol

The synthesis of the smart probe **CHMC-thiol** was accomplished in four steps as shown in Scheme 1. Starting material **1** is commercially available. The intermediate aldehyde **2** was

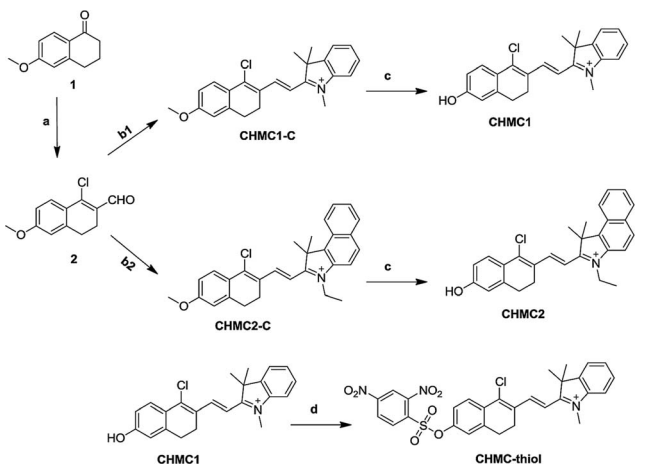

Scheme 1 Synthesis of compounds **CHMC-thiol** and some controls **CHMC1,2**. *Reagents and conditions*: (a) DMF/$POCl_3$, 5 h; (b1) 1-butanol–benzene (7 : 3), indolium salt, 90 °C, 5 h; (b2) 1-butanol–benzene (7 : 3), benz[e]indolium salt, 90 °C, 5 h; (c) BBr_3, dry CH_2Cl_2, 0 °C, overnight. (d) Cs_2CO_3, CH_2Cl_2, 2,4-dinitrobenzenesulfonyl chloride, room temperature, 5 h.

prepared by the Vilsmeier reaction, and it was further used to synthesize the compounds **CHMC1-C** and **CHMC2-C** by the Knoevenagel condensation without purification.

Treatment of **CHMC1-C** and **CHMC2-C** with BBr_3 in dry CH_2Cl_2 afforded the controls **CHMC1** and **CHMC2**, respectively. Then, the **CHMC1** dye was reacted with 2,4-dinitrobenzenesulfonyl chloride under basic conditions to provide the target compound **CHMC-thiol**. The detailed synthetic procedures are presented in the Experimental section. All new compounds were carefully characterized by ^{1}H NMR, ^{13}C NMR and HRMS (ESI†).

Photophysical properties of fluorescent dyes CHMC1,2

To support our design concept of the new fluorescent probe **CHMC-thiol**, we proceeded to investigate the optical properties of the **CHMC** dyes. The absorption and emission profiles of compounds **CHMC1**, **CHMC2**, **CHMC1-C** and **CHMC2-C** in distinct solvents (*i.e.* EtOH, PBS) are shown in Fig. S1 and Table S1.† First, we investigated the spectral properties of **CHMC1**, **CHMC2**, **CHMC1-C** and **CHMC2-C** dyes in the protic solvent EtOH. The absorption spectra of **CHMC1** and **CHMC2** (5 μM) in EtOH possess a broad absorption band due to the various vibrational and rotational states, typical of the merocyanine dyes. Notably, **CHMC1** and **CHMC2** have a maximum absorption peak at around 670–690 nm in EtOH, in the NIR region, with large molar absorption coefficient (>10^5). Fluorescence spectra of **CHMC1** and **CHMC2** exhibit strong fluorescence with a maximum emission peak at around 695 and 714 nm, respectively. This behavior of **CHMC1** and **CHMC2** NIR dyes is in good agreement with that of the classic NIR carbocyanine dyes. The compounds **CHMC1-C** and **CHMC2-C**, which bear no key hydroxyl group, display weak fluorescence. Thus, these data suggest that the optical properties of **CHMC1** and **CHMC2** dyes can be regulated by alkylation on the hydroxyl group.

To get more insight to the hydroxyl chemical handle in **CHMC** dyes, we examined the pH effect on the photophysical properties of **CHMC1** and **CHMC2** dyes in PBS. The standard pH titrations on the compound **CHMC1** (5 μM) were performed in aqueous solution (containing 10% EtOH as a co-solvent). With the enhancement of pH values from 3.0 to 10.0, the absorption peak of **CHMC1** at around 500 nm significantly diminishes, and simultaneously a new red-shifted absorption band at around 630 nm is observed (Fig. S2†). There is a well-defined isosbestic point at 543 nm in the absorption spectra, suggesting the presence of two species in equilibrium. The red-shift in the absorption spectra with increase of pH can be explained due to the deprotonation of the **CHMC1** dye. The pH-dependent absorption spectra of **CHMC2** (Fig. S3†) exhibit a similar trend to those of **CHMC1** with the enhancement of pH values from 3.0 to 10.0.

The fluorescence emission spectrum of **CHMC1** at pH 3.0 displays an emission band with a maximum at 616 nm (Fig. 3a). Deprotonation of **CHMC1** increases the electron donating ability of the hydroxyl group and therefore results in a *ca.* 64 nm red-shift in the emission spectra from 616 to 680 nm (Fig. 3a). The pH-dependent emission spectra of **CHMC2** (Fig. 3c) display

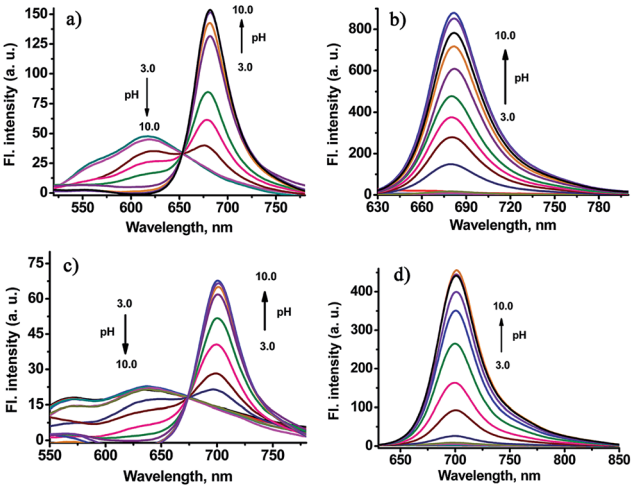

Fig. 3 (a) pH-Dependence of the emission spectra of compound **CHMC1** (5 μM) with the arrows indicating the change of the emission intensities with pH enhancement from 3 to 10, excitation at 480 nm; (b) pH-dependence of the emission spectra of compound **CHMC1** (5 μM) with the arrows indicating the change of the emission intensities with pH enhancement from 3 to 10, excitation at 630 nm; (c) pH-dependence of the emission spectra of compound **CHMC2** (5 μM) with the arrows indicating the change of the emission intensities with pH enhancement from 3 to 10, excitation at 480 nm; (d) pH-dependence of the emission spectra of compound **CHMC2** (5 μM) with the arrows indicating the change of the emission intensities with pH enhancement from 3 to 10, excitation at 630 nm.

a red-shift in the emission spectra from 635 to 700 nm. The analysis of emission intensity changes at 680 nm for **CHMC1** and 700 nm for **CHMC2** as a function of pH by using the Henderson–Hasselbalch-type mass action equation yields pK_a values of 7.05 and 7.15, respectively.[13] The ratios of fluorescence intensities at 680 and 616 nm (I_{680}/I_{616}) of **CHMC1** show a dramatic change from 0.43 at pH 3.0 to 52.3 at pH 10.0 (Fig. S4†), a nearly 121-fold variation in the emission ratios. Similarly, the emission ratios of **CHMC2** (I_{700}/I_{635}) exhibit a 258-fold change in the emission ratios (Fig. S5†).

When excited at 630 nm, the emission band of **CHMC1** centered at 680 nm rises as the pH value increases, and it shows a 45-fold fluorescence intensity enhancement (Fig. 3b and S6a†). The pH-dependent emission spectra of **CHMC2** exhibits the similar trend with pH values increased from 3.0 to 10.0 (Fig. 3d and S6b†). These results indicate that the optical properties of the two-chemical-handle NIR dyes **CHMC1** and **CHMC2** can be controlled by modifications on the hydroxyl handle. Thus, as designed, **CHMC** dyes still maintain the tunable hydroxyl handle, just like the previously developed **HD** NIR dyes.

Sensing of CHMC1 and CHMC2 to high and low concentration ranges of thiols

Like chloro-substituted cyanine, the chloro moiety of **CHMC1** and **CHMC2** may also provide the dyes with a chemical handle for substitution at the central ring. For further proof of our design concept of the fluorescent probe **CHMC-thiol**, we must

examine the possibility of **CHMC1** and **CHMC2** to detect thiols in PBS using the chloro group. In preliminary experiments, we first evaluated the capability of **CHMC1** and **CHMC2** to detect thiols (represented by Cys) in PBS in the presence of a low concentration range of Cys. As shown in Fig. S7 and S8,† addition of a low concentration range of Cys (0–35 μM) induces no marked fluorescence changes after 1 h.

To further understand the ability of **CHMC1** and **CHMC2** to sense Cys, these two dyes were incubated with a high concentration range of Cys (35–500 μM). As shown in Fig. 4a, upon excitation at 550 nm, the free **CHMC1** shows the emission peak at 680 nm. However, upon addition of a high concentration range of Cys, the emission peak at 680 nm gradually decreases, and a new emission band at 625 nm appears. Consistently, a marked blue-shift from 643 to 541 nm is noted in the absorption spectra upon treatment of **CHMC1** with Cys (Fig. S9†). When adding 100 equiv. Cys, the ratios of fluorescence intensities at 625 nm and 680 nm (I_{625}/I_{680}) of **CHMC1** show a dramatic change from 0.26 to 7.7, a nearly 29-fold enhancement in the emission ratio. Similarly, the ratios of compound **CHMC2** (I_{642}/I_{700}) exhibit a 47-fold change (Fig. 4b). The mass spectrometry analyses confirm that the ratiometric fluorescence changes in the emission profiles is due to the substitution reaction by the thiolate of Cys and followed by intramolecular rearrangement (Fig. S10†). The results indicate that, as for the chloro-substituted cyanine dye, the two-chemical-handle NIR dyes **CHMC1** and **CHMC2** still retain the chloro moiety as the effective interaction site for Cys. In other words, as designed, **CHMC1** and **CHMC2** can be employed to sense a high concentration range of Cys by the chloro group. Notably, the threshold of high concentration range of Cys which elicits the ratio signal in fluorescence is well within the physiological concentration range of Cys (30–200 uM).[14]

Sensing of the probe CHMC-thiol to high and low concentration ranges of thiols in PBS

In order to test the design strategy of the probe **CHMC-thiol**, we evaluated its capability to detect biological thiols (represented by Cys) in PBS. As designed, the free probe is almost non-fluorescent in PBS (Fig. 5a). However, addition of a low concentration range of Cys (0–50 μM) induces significant variations in the fluorescence spectra at 680 nm. In good agreement, a marked red-shift from 442 to 657 nm is present in the absorption spectra upon treatment of the probe with Cys (Fig. S11a†). By contrast, addition of a high concentration range of Cys (50–500 μM) elicits a fluorescence ratiometric response in the fluorescence spectra (Fig. 5b). The corresponding absorption spectra upon treatment of the probe with Cys are shown in Fig. S11b.†

To further estimate the ability of the probe **CHMC-thiol**, we also examined the response of the probe at a different concentration, *i.e.* 10 μM. As shown in Fig. S12,† the results are very similar to those of the probe at 5 μM. Taken together, the studies indicate that the probe **CHMC-thiol** has distinct modes of fluorescence signals towards the different concentration ranges of thiols. The probe exhibits a turn-on mode of the fluorescence signal to the low concentration range of thiols at 680 nm, while displaying a ratiometric mode of the fluorescence signal to the high concentration range of thiols. Thus, the emission peak at 625 nm may be considered as an important marker for the concentration range of Cys (Fig. 5d). To the best of our knowledge, this represents the first fluorescent probe which can sense low and high concentration ranges of thiols with different modes of the fluorescence signals.

Based on the above vital findings, a possible mechanistic pathway for sensing thiols is proposed in Scheme 2. The probe **CHMC-thiol** has distinct response pathways towards different concentration ranges of thiols. On the one hand, upon reaction with a low concentration range of Cys, the fluorescence turn-on is due to the thiol-mediated removal of the 2,4-dinitrobenzenesulfonate moiety. Both mass spectrometry (Fig. S13†) and NMR (Fig. S14†) analyses confirm the formation of **CHMC1**. In addition, from the fluorescence point of view, the

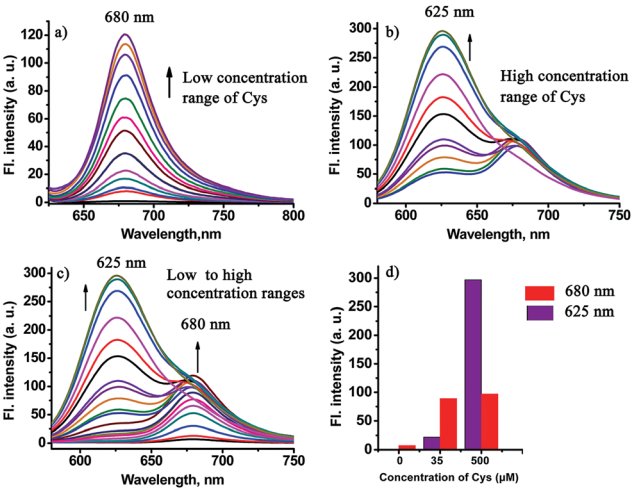

Fig. 5 (a) Fluorescence spectra of the probe **CHMC-thiol** (5 μM) in the presence of a low concentration range of Cys (0–50 μM); (b) fluorescence spectra of the probe **CHMC-thiol** (5 μM) in the presence of a high concentration range of Cys (50–500 μM); (c) fluorescence spectra of the probe **CHMC-thiol** (5 μM) in the presence of low to high concentration ranges of Cys (0–500 μM); (d) fluorescence intensity at 680 or 625 nm of the probe **CHMC-thiol** (5 μM) in the presence of representative concentrations of Cys (0, 35, 500 μM). All spectra were obtained after adding the analyte for 1 h and excitation at 550 nm.

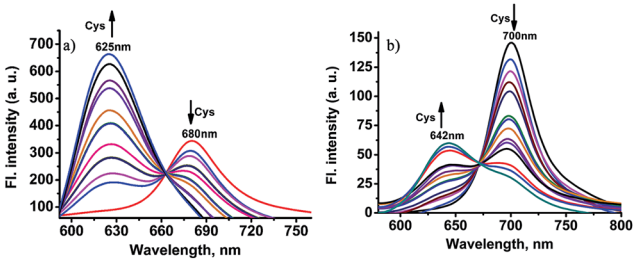

Fig. 4 (a) Fluorescence spectra of **CHMC1** (5 μM) in the aqueous buffer in the presence of a high concentration range of Cys (35–500 μM), excitation at 550 nm; (b) fluorescence spectra of the probe **CHMC2** (5 μM) in aqueous buffer in the presence of a high concentration range of Cys (35–500 μM), excitation at 550 nm.

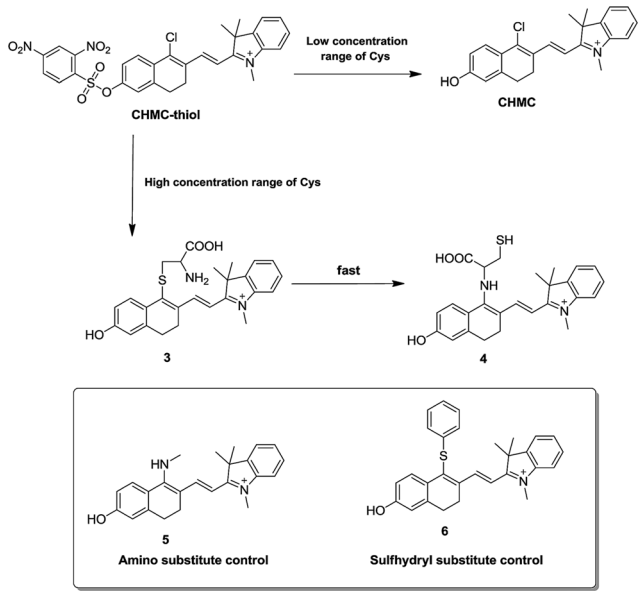

Scheme 2 The proposed reaction mechanism of **CHMC-thiol** with biological thiols (represented by Cys) and the structures of the amino and sulfhydryl substituted controls **5** and **6**.

normalized emission of the probe **CHMC-thiol** reaction with the low concentration range of Cys (Fig. S15a†) highly resembles that of **CHMC1** (Fig. S15b†). On the other hand, in the presence of a high concentration range of Cys, the chloro group in **CHMC-thiol** is initially replaced by the thiol group of Cys to produce the 4-sulfhydryl intermediate **3**, and the subsequent intramolecular SNAr substitution of the sulfhydryl moiety by the amino group leads to the formation of the 4-amino product **4**.[2c,2f,12,15] This process is consistent with the results of mass spectrometry (Fig. S16†) and NMR analyses (Fig. S17†). To further confirm that the final product is the 4-amino product **4** instead of the 4-sulfhydryl intermediate **3**, we further synthesized compounds **5** and **6** as the amino and sulfhydryl substituted controls, respectively (Scheme 2). The spectral studies indicate that the emission profile of the probe **CHMC-thiol** reaction with high concentration range of Cys highly resembles that of the control **5** instead of **6** (Fig. S18†). Thus, taken together, these data corroborate the sensing mechanism of **CHMC-thiol** in the presence of low and high concentration ranges of Cys as proposed in Scheme S2.†

We also evaluated the capability of **CHMC-thiol** to detect other small-molecular-weight biological thiols (Hcy and GSH). The titrations of the novel probe **CHMC-thiol** (5 μM) with Hcy were conducted in PBS (pH 7.4, containing 10% EtOH as a cosolvent). The probe **CHMC-thiol** exhibits a similar behavior towards Hcy as found for Cys. Upon reaction with a low concentration range of Hcy, the fluorescence turn-on at 680 nm is due to the thiol-mediated removal of the 2,4-dinitrobenzenesulfonate moiety. However, on addition of a high concentration range of Hcy, a ratiometric response is observed owing to nucleophilic substitution followed by an intramolecular rearrangement (Fig. S19 and Scheme S1†). Hcy is a potential interferent at certain conditions for the detection of Cys due to the structural and chemical similarity between them. In the presence of a low concentration range of GSH, the probe **CHMC-thiol** shows a similar trend to Cys and Hcy. However, the treatment of the probe with a high concentration range of GSH only produces the 4-sulfhydryl product due to the steric hindrance, which leads to a 10 nm redshift in the emission spectra (Fig. S20 and Scheme S2†). These results are in good agreement with those reported in the literature.[2c,2f,12,15]

To examine the selectivity, the probe **CHMC-thiol** (5 μM) was treated with various biologically relevant species (*e.g.*, representative anions, metal ions, reactive oxygen species, reactive nitrogen species, reducing agents) in aqueous buffer. As shown in Fig. 6, addition of representative anions (Cl^-, Br^-, I^-, AcO^-, N_3^-, CN^-, CO_3^{2-}, NO_2^-) at 1 mM, metal ions (K^+, Mg^{2+}, Ca^{2+}, Zn^{2+}) at 1 mM, reactive oxygen and nitrogen species (H_2O_2, ClO^-, NO), and reducing agents (ascorbic acid, Na_2S) at biologically relevant concentrations induces no marked fluorescence enhancement at 680 nm. By contrast, upon treatment of thiols with the probe, a large fluorescence signal was observed at 680 nm (Fig. 6a). The fluorescence signals at 625 nm (Fig. 6b) are consistent with those at 680 nm (Fig. 6a). Thus, these data demonstrate that the probe **CHMC-thiol** has a high selectivity for thiols over other biological species tested at biologically relevant concentrations, suggesting that the probe **CHMC-thiol** is favorable for studies of biological thiols in biological systems.

Kinetic studies of the probe CHMC-thiol

The time course of the probe **CHMC-thiol** in the presence of thiols (represented by Cys) is displayed in Fig. 7. The response of the 2,4-dinitrobenzenesulfonate moiety (the high-sensitivity site)

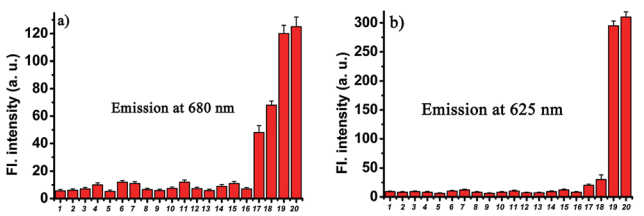

Fig. 6 (a) Fluorescence responses of the probe **CHMC-thiol** (5 μM) to various biologically relevant species in aqueous buffer. Red bars represent the addition of an excess of the representative anions, metal ions, reactive oxygen species, reactive nitrogen species, reducing agents, small-molecule thiols. (Cl^-, Br^-, I^-, AcO^-, N_3^-, CN^-, CO_3^{2-}, NO_2^-) at 1 mM, metal ions (K^+, Mg^{2+}, Ca^{2+}, Zn^{2+}) at 1 mM, reactive oxygen and nitrogen species (H_2O_2, OCl^-, NO, Na_2S) at 100 μM. Ascorbic acid, GSH, Hcy and Cys at 1 mM. (1) Cl^-, (2) Br^-, (3) I^-, (4) AcO^-, (5) N_3^-, (6) CN^-, (7) CO_3^{2}, (8) NO_2^-, (9) Mg^{2+}, (10) K^+, (11) Zn^{2+}, (12) Ca^{2+}, (13) H_2O_2, (14) ClO^-, (15) NO, (16) ascorbic acid, (17) Na_2S, (18) GSH, (19) Hcy, (20) Cys. Excitation at 550 nm and emission at 680 nm; (b) fluorescence responses of the probe **CHMC-thiol** (5 μM) to various biologically relevant species in aqueous buffer. Cl^-, Br^-, I^-, AcO^-, N_3^-, CN^-, CO_3^{2-}, NO_2^-) at 1 mM, metal ions (K^+, Mg^{2+}, Ca^{2+}, Zn^{2+}) at 1 mM, reactive oxygen and nitrogen species (H_2O_2, OCl^-, NO) at 100 μM. Ascorbic acid, GSH, Hcy and Cys at 1 mM. (1) Cl^-, (2) Br^-, (3) I^-, (4) AcO^-, (5), N_3^-, (6) CN^-, (7) CO_3^{2}, (8) NO_2^-, (9) Mg^{2+}, (10) K^+, (11) Zn^{2+}, (12) Ca^{2+}, (13) H_2O_2, (14) ClO^-, (15) NO, (16) ascorbic acid, (17) Na_2S, (18) GSH, (19) Hcy, (20) Cys. Excitation at 550 nm and emission at 625 nm. Data were expressed as mean ± SD of three experiments.

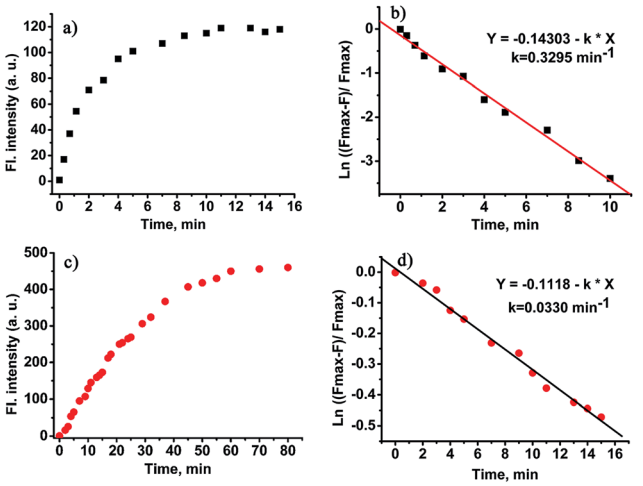

Fig. 7 (a) Reaction-time profiles of **CHMC-thiol** (5.0 μM) in the presence of 100 μM Cys (■) at 680 nm; (b) pseudo-first-order kinetic plot of the reaction of the probe **CHMC-thiol** (5 μM) with Cys (100 μM) at 680 nm in pH 7.4, 25 mM PBS. Slope = 0.3295 min^{-1}; (c) reaction-time profiles of **CHMC-thiol** (5.0 μM) in the presence of 500 μM Cys (■) at 625 nm; (d) pseudo-first-order kinetic plot of the reaction of the probe **CHMC-thiol** (5 μM) with Cys (500 μM) at 625 nm in pH 7.4, 25 mM PBS. Slope = 0.0330 min^{-1}.

of **CHMC-thiol** to Cys is fast, and the reaction is complete within 10 min at 680 nm (Fig. 7a). The pseudo-first-order rate constant of the high-sensitivity site is calculated to be $k = 0.3295\ min^{-1}$ for Cys at 680 nm (Fig. 7b). By contrast, the response of the chloro group (the low sensitivity site) of **CHMC-thiol** to Cys is slower than the 2,4-dinitrobenzenesulfonate moiety, and the reaction is complete within 60 min at 625 nm (Fig. 7c). The pseudo-first-order rate constant of the second site is calculated to be $k = 0.033\ min^{-1}$ for Cys at 625 nm (Fig. 7d). The pseudo-first-order rate constant of the high sensitivity site is about 10 times that of the low sensitivity site. It is important to note that such a large difference in the pseudo-first-order rate constants of the two sensing sites is highly desirable for the development of concentration range-dependent fluorescent probes.

Imaging of the CHMC-thiol to different concentration ranges of thiols in live cells

Notably, the threshold of the low and high concentration ranges of the fluorescent probes **CHMC-thiol** is well within the physiological concentration range of Cys (30–200 μM).[14] For preliminary fluorescence imaging applications, the probe **CHMC-thiol** was incubated with living HeLa cells pretreated with or without *N*-ethylmaleimide (as a thiol blocking agent). As shown in Fig. 8g, the cells treated only with the probe exhibit strong fluorescence in the red channel. However, when the cells are pretreated with *N*-ethylmaleimide, then incubated with **CHMC-thiol**, much weaker fluorescence in the red channel is observed (Fig. 8c). To further study the ability of the probe **CHMC-thiol** for imaging different concentration ranges of thiols in living cells, the cells were incubated with Cys (100 μM) for 30 min, and then treated with the probe **CHMC-thiol** (5 μM) for another 30 min. In such a case, the cells exhibit intense fluorescence in the orange

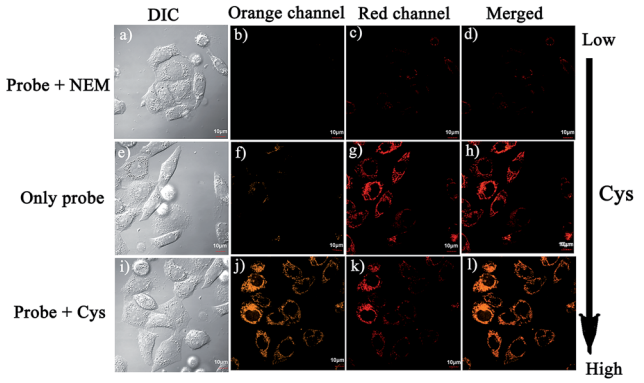

Fig. 8 Bright-field and fluorescence images of HeLa cells stained with the **CHMC-thiol**: (a–d) bright-field and fluorescence images of the cells incubated with *N*-ethylmaleimide, and then co-incubated with **CHMC-thiol** for 30 min: (e–h) bright-field and fluorescence images of cells incubated only with the probe for 30 min: (i–l) bright-field and fluorescence images of cells incubated with Cys for 30 min, and then treated with the probe for 30 min: the orange and red channels are corresponding to the emission windows of 580–640, and 650–750 nm, respectively. Scale bar = 10 μm.

channel (Fig. 8j). By contrast, the cells incubated with only the probe display almost no fluorescence in the orange channel (Fig. 8f). Thus, in the living cells, the probe shows a turn-on mode in the presence of the low concentration range of Cys (Fig. 8c and g) and a ratiometric mode in the presence of the high concentration range of Cys (Fig. 8f, g, j and k, and 9). Similar results are noted when the probe is treated with another type of cells, MCF-7 cells (Fig. S21†). These imaging data in the living cells are consistent with the results in solution (Fig. 5). Thus, as designed, the probe **CHMC-thiol** is cell membrane permeable and can report low and high concentration ranges of thiols with distinct modes of fluorescence signals in the living cells.

Imaging of CHMC-thiol to different concentration ranges of thiols in live animals

Based on the above studies, the prominent features of the probe **CHMC-thiol** include excellent NIR photophysical properties,

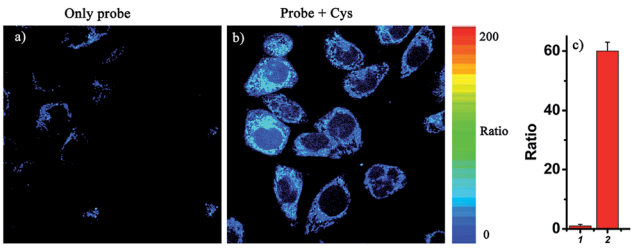

Fig. 9 Pseudo-colored ratiometric images (F_{orange}/F_{red}) of thiols in HeLa cells. (a) Ratio image (F_{orange}/F_{red}) of the cells incubated only with the probe **CHMC-thiol** (5 μM) for 30 min; (b) ratio image (F_{orange}/F_{red}) of the cells incubated with Cys (100 μM) for 30 min, and then treated with the probe (5 μM) for another 30 min; (c) average F_{orange}/F_{red} intensity ratios in (a, b). The orange and red channels are corresponding to the emission windows of 580–640, and 650–750 nm, respectively. Data are expressed as mean ± SD of three experiments.

two reactive sites with different sensitivity and excellent selectivity. In particular, the threshold of the low and high concentration ranges of **CHMC-thiol** is well located in the physiological concentration range of Cys (30–200 μM).[14] These favorable attributes encourage us to further investigate the suitability of the probe for detecting different concentration ranges of thiols with distinct modes of fluorescence signals in the context of living mice. The Kunming mice were divided into three groups (Fig. 10). One group was given saline (100 μL) in the peritoneal cavity, followed by intraperitoneal (i.p.) injection with **CHMC-thiol** (20 μM, in 20 μL DMSO). The second group was given an i.p. injection of *N*-ethylmaleimide (1 mM, in 100 μL saline), and followed by i.p. injection with **CHMC-thiol** (20 μM, in 20 μL DMSO) as the negative control experiment. The third group was given an i.p. injection of Cys (100 μM, in 100 μL saline), and followed by i.p. injection with **CHMC-thiol** (20 μM, in 20 μL DMSO). As shown in Fig. 10b, the mice treated with only the probe exhibit a much higher fluorescence readout (pseudocolor) than the mice treated with NEM (Fig. 10a) in the red channel. In addition, the mice treated with only the probe display a much higher fluorescence readout (pseudocolor) than the mice incubated with NEM and the probe (Fig. 10d and e) in the orange channel, but less than the mice incubated with Cys and the probe (Fig. 10f). Thus, the probe exhibits a turn-on mode to the low concentration range of Cys (Fig. 10a, b and g(1, 2)) and a ratiometric signal to the high concentration range of Cys (Fig. 10b, c, e, f and h). Notably, the imaging data in the living animals are consistent with both the results in the solution (Fig. 5) and the living cells (Fig. 8). Thereby, these results demonstrate that the robust fluorescent probe **CHMC-thiol** can image the different concentration ranges of thiols with distinct modes of fluorescence signals in the living animals, for the first time.

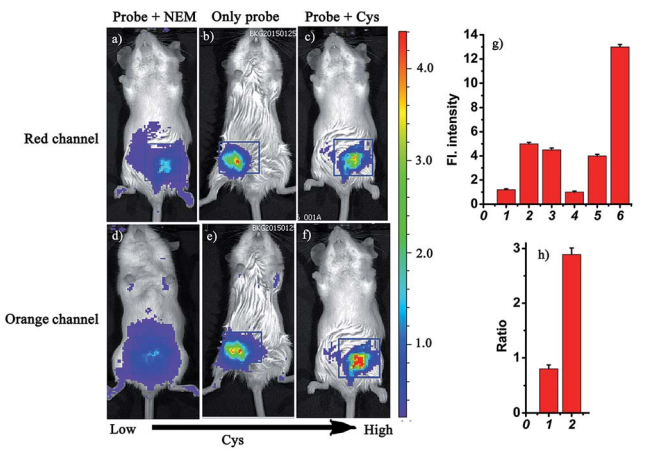

Fig. 10 Representative fluorescent images (pseudo-color) of thiols (Cys) in the mice: (a) and (d) the mice were given an i.p. injection of *N*-ethylmaleimide and followed by injection with **CHMC-thiol**; (b) and (e) only the **CHMC-thiol** was injected in the peritoneal cavity of the mice; (c) and (f) the mice were given an i.p. injection of Cys and followed by an i.p. injection with **CHMC-thiol**. (g) Quantification of the fluorescence emission intensity from the abdominal area of the mice of groups a(1), b(2), c(3); d(4), e(5), f(6); (h) average F_{orange}/F_{red} intensity ratios of the only probe group (1) and probe + Cys group (2). The mice were imaged with an excitation filter of 550 nm and the orange and red channels are corresponding to the emission windows of 580–640 nm, and 650–750 nm, respectively. Data were expressed as mean ± SD of three experiments.

Conclusions

In summary, we have described a unique approach for the development of concentration range-dependent fluorescent probes. Based on the proposed strategy, we have synthesized the first concentration range-dependent NIR fluorescent probe, **CHMC-thiol**, which, interestingly, is capable of monitoring the low concentration range of thiols with a turn-on fluorescence signal and providing a ratiometric fluorescence response to the high concentration range of thiols. We have further demonstrated that the new probe can be employed to sense the changes in the thiol concentration ranges with distinct modes of fluorescence signals in both living cells and living animals. In addition, the innovative NIR dye, **CHMC**, is superior to the traditional chloro-substituted cyanine and the recently developed **HD** NIR dyes with retaining both the regulation sites of these two types of NIR dyes. We believe that **CHMC**, which intrinsically bears two chemical handles, may serve as a useful fluorescent platform for the design of the concentration range-dependent NIR fluorescent probes as powerful molecular tools for biological and clinical investigations in living systems.

Acknowledgements

Funding was partially provided by NSFC (21172063, 21472067) and the startup fund of University of Jinan.

Notes and references

1 (*a*) X. Chen, Y. Zhou, X. Peng and J. Yoon, *Chem. Soc. Rev.*, 2010, **39**, 2120; (*b*) C. Yin, F. Huo, J. Zhang, R. Martínez-Máñez, Y. Yang, H. Lv and S. Li, *Chem. Soc. Rev.*, 2013, **42**, 6032; (*c*) H. S. Jung, X. Chen, J. S. Kim and J. Yoon, *Chem. Soc. Rev.*, 2013, **42**, 6019; (*d*) L.-Y. Niu, Y.-Z. Chen, H.-R. Zheng, L.-Z. Wu, C.-H. Tung and Q.-Z. Yang, *Chem. Soc. Rev.*, 2015, **44**, 6143.

2 (*a*) O. Rusin, N. N. St Luce, R. A. Agbaria, J. O. Escobedo, S. Jiang, I. M. Warner, F. B. Dawan, K. Lian and R. M. Strongin, *J. Am. Chem. Soc.*, 2004, **126**, 438; (*b*) X. Yang, Y. Guo and R. M. Strongin, *Angew. Chem., Int. Ed.*, 2011, **50**, 10690; (*c*) L. Y. Niu, Y. S. Guan, Y. Z. Chen, L. Z. Wu, C. H. Tung and Q. Z. Yang, *J. Am. Chem. Soc.*, 2012, **134**, 18928; (*d*) J. Yin, Y. Kwon, D. Kim, D. Lee, G. Kim, Y. Hu, J.-H. Ryu and J. Yoon, *J. Am. Chem. Soc.*, 2014, **136**, 5351; (*e*) S. Y. Lim, K. H. Hong, D. I. Kim, H. Kwon and H. J. Kim, *J. Am. Chem. Soc.*, 2014, **136**, 7018; (*f*) J. Liu, Y. Q. Sun, Y. Huo, H. Zhang, L. Wang, P. Zhang and W. Guo, *J. Am. Chem. Soc.*, 2014, **136**, 574; (*g*) Z. Guo, S. W. Nam, S. Park and J. Yoon, *Chem. Sci.*, 2012, **3**, 2760.

3 (*a*) X. Lou, Y. Hong, S. Chen, C. W. T. Leung, N. Zhao, B. Situ, J. W. Y. Lam and B. Z. Tang, *Sci. Rep.*, 2014, **4**, DOI: 10.1038/srep04272; (*b*) H. S. Hewage and E. V. Anslyn, *J. Am. Chem.*

Soc., 2009, **131**, 13099; (*c*) C. S. Lim, G. Masanta, H. J. Kim, J. H. Han, H. M. Kim and B. R. Cho, *J. Am. Chem. Soc.*, 2011, **133**, 11132; (*d*) M. Zhang, M. Yu, F. Li, M. Zhu, M. Li, Y. Gao, T. Yi and C. Huang, *J. Am. Chem. Soc.*, 2007, **129**, 10322; (*e*) B. Tang, Y. Xing, P. Li, N. Zhang, F. Yu and G. Yang, *J. Am. Chem. Soc.*, 2007, **129**, 11666; (*f*) Y. H. Ahn, J. S. Lee and Y. T. Chang, *J. Am. Chem. Soc.*, 2007, **129**, 4510; (*g*) J. Shao, H. Sun, H. Guo, S. Ji, J. Zhao, W. Wu and T. D. James, *Chem. Sci.*, 2012, **3**, 1049; (*h*) R. Wang, L. Chen, P. Liu, Q. Zhang and Y. Wang, *Chem.–Eur. J.*, 2012, **18**, 11343; (*i*) F. Wang, Z. Guo, X. Li, X. Li and C. Zhao, *Chem.–Eur. J.*, 2014, **20**, 11471.

4 (*a*) L. D. Lavis and R. T. Raines, *ACS Chem. Biol.*, 2014, **9**, 855; (*b*) B. A. Smith, W. J. Akers, W. M. Leevy, A. J. Lampkins, S. Z. Xiao, W. Wolter, M. A. Suckow, S. Achilefu and B. D. Smith, *J. Am. Chem. Soc.*, 2010, **132**, 67; (*c*) K. Kundu, S. F. Knight, N. Willett, S. Lee, W. R. Taylor and N. Murthy, *Angew. Chem., Int. Ed.*, 2009, **48**, 299; (*d*) N. Karton-Lifshin, L. Albertazzi, M. Bendiko, P. S. Baran and D. Shabat, *J. Am. Chem. Soc.*, 2012, **134**, 20412; (*e*) W. Xuan, C. Sheng, Y. Cao, W. He and W. Wang, *Angew. Chem., Int. Ed.*, 2012, **51**, 2282; (*f*) X. Wu, M. Yu, B. Lin, H. Xing, J. Han and S. Han, *Chem. Sci.*, 2015, **6**, 798; (*g*) J. J. Hu, N.-K. Wong, S. Ye, X. Chen, M.-Y. Lu, A. Q. Zhao, Y. Guo, A. C.-H. Ma, A. Y.-H. Leung, J. Shen and D. Yang, *J. Am. Chem. Soc.*, 2015, **137**, 6837; (*h*) C. Huang, T. Jia, M. Tang, Q. Yin, W. Zhu, C. Zhang, Y. Yang, N. Jia, Y. Xu and X. Qian, *J. Am. Chem. Soc.*, 2014, **136**, 14237.

5 (*a*) K. Kiyose, H. Kojima and T. Nagano, *Chem.–Asian J.*, 2008, **3**, 506; (*b*) M. Lin, B. Fimmel, K. Radacki and F. Würthner, *Angew. Chem., Int. Ed.*, 2011, **50**, 10847; (*c*) G. M. Fischer, E. Daltrozzo and A. Zumbusch, *Angew. Chem., Int. Ed.*, 2011, **50**, 1406; (*d*) T. Hirayamaa, G. C. Van de Bittnera, L. W. Grayb, S. Lutsenkob and C. J. Chang, *Proc. Natl. Acad. Sci. U. S. A.*, 2012, **109**, 2228; (*e*) M. Cui, M. Ono, H. Watanabe, H. Kimura, B. Liu and H. Saji, *J. Am. Chem. Soc.*, 2014, **136**, 3388; (*f*) A. T. Wrobel, T. C. Johnstone, A. Deliz-Liang, S. J. Lippard and P. Rivera-Fuentes, *J. Am. Chem. Soc.*, 2014, **136**, 4697.

6 (*a*) M. Schäerling, *Angew. Chem., Int. Ed.*, 2012, **51**, 3532; (*b*) Y. Yang, Q. Zhao, W. Feng and F. Li, *Chem. Rev.*, 2013, **113**, 192; (*c*) X. Li, X. Gao, W. Shi and H. Ma, *Chem. Rev.*, 2014, **114**, 590; (*d*) R. Guliyev, A. Coskun and E. U. Akkaya, *J. Am. Chem. Soc.*, 2009, **131**, 9007; (*e*) Y. Ueno, J. Jose, A. Loudet, C. Pérez-Bolívar, P. Anzenbacher Jr. and K. Burgess, *J. Am. Chem. Soc.*, 2011, **133**, 51; (*f*) E. Heyer, P. Retailleau and R. Ziessel, *Org. Lett.*, 2014, **16**, 2330; (*g*) F. Yu, P. Li, B. Wang and K. Han, *J. Am. Chem. Soc.*, 2013, **135**, 7674; (*h*) J. Ling, G. Naren, J. Kelly, T. S. Moody and A. P. de Silva, *J. Am. Chem. Soc.*, 2015, **137**, 3763.

7 (*a*) M. H. Lee, B. Yoon, J. S. Kim and J. L. Sessler, *Chem. Sci.*, 2013, **4**, 4121; (*b*) X. Wang, L. Cui, N. Zhou, W. Zhu, R. Wang, X. Qian and Y. Xu, *Chem. Sci.*, 2013, **4**, 2936; (*c*) C. Liu, W. Chen, W. Shi, B. Peng, Y. Zhao, H. Ma and M. Xian, *J. Am. Chem. Soc.*, 2014, **136**, 7257; (*d*) Z. Huang, S. Yu, K. Wen, X. Yu and L. Pu, *Chem. Sci.*, 2014, **5**, 3457; (*e*) D. R. Rooker and D. Buccella, *Chem. Sci.*, 2015, **6**, 6456; (*f*) Y. You and W. Nam, *Chem. Sci.*, 2014, **5**, 4123; (*g*) Y.-J. Huang, W.-J. Ouyang, X. Wu, Z. Li, J. S. Fossey, T. D. James and Y.-B. Jiang, *J. Am. Chem. Soc.*, 2013, **135**, 1700; (*h*) J. Zhou, L. Li, W. Shi, X. Gao, X. Li and H. Ma, *Chem. Sci.*, 2015, **6**, 4884; (*i*) Q. Zhao, X. Zhou, T. Cao, K. Y. Zhang, L. Yang, S. Liu, H. Liang, H. Yang, F. Li and W. Huang, *Chem. Sci.*, 2015, **6**, 1825.

8 (*a*) H. Komatsu, T. Miki, D. Citterio, T. Kubota, Y. Shindo, Y. Kitamura, K. Oka and K. Suzuki, *J. Am. Chem. Soc.*, 2005, **127**, 10798; (*b*) L. Yuan, W. Lin, Y. Xie, B. Chen and S. Zhu, *J. Am. Chem. Soc.*, 2012, **134**, 1305; (*c*) X. Gao, X. Li, L. Li, J. Zhou and H. Ma, *Chem. Commun.*, 2015, **51**, 9388.

9 (*a*) L. Strekowski, M. Lipowska and G. Patonay, *J. Org. Chem.*, 1992, **57**, 4578; (*b*) X. Peng, F. Song, E. Lu, Y. Wang, W. Zhou, J. Fan and Y. Gao, *J. Am. Chem. Soc.*, 2005, **127**, 4170.

10 L. Yuan, W. Lin, S. Zhao, W. Gao, B. Chen, L. He and S. Zhu, *J. Am. Chem. Soc.*, 2012, **134**, 13510.

11 (*a*) H. Maeda, H. Matsuno, M. Ushida, K. Katayama and K. Saeki, *Angew. Chem., Int. Ed.*, 2005, **44**, 2922; (*b*) J. Zhang, A. Shibata, M. Ito, S. Shuto, Y. Ito, B. Mannervik, H. Abe and R. Morgenstern, *J. Am. Chem. Soc.*, 2011, **133**, 14109; (*c*) W. Jiang, Q. Fu, H. Fan, J. Ho and W. Wang, *Angew. Chem., Int. Ed.*, 2007, **46**, 8445; (*d*) X. Liu, W. Zhang, C. Li, W. Zhou, Z. Li, M. Yu and L. Weia, *RSC Adv.*, 2015, **5**, 4941.

12 (*a*) L.-Y. Niu, H.-R. Zheng, Y.-Z. Chen, L.-Z. Wu, C.-H. Tung and Q.-Z. Yang, *Analyst*, 2014, **139**, 1389; (*b*) X. Wang, J. Lv, X. Yao, Y. Li, F. Huang, M. Li and B. Tang, *Chem. Commun.*, 2014, **50**, 15439.

13 The pK_a was calculated according to the Henderson–Hasselbalch-type mass action equation ($\log[(F_{max} - F)/(F - F_{min})] = pK_a - pH$).

14 (*a*) T. K. Chung, M. A. Funk and D. H. Baker, *J. Nutr.*, 1990, **120**, 158; (*b*) S. Park and J. A. Imlay, *J. Bacteriol.*, 2003, **185**, 1942.

15 (*a*) J. Liu, Y.-Q. Sun, H. Zhang, Y. Huo, Y. Shi and W. Guo, *Chem. Sci.*, 2014, **5**, 3183; (*b*) Y. Kim, S. V. Mulay, Mi. Choi, S. B. Yu, S. Jon and D. G. Churchill, *Chem. Sci.*, 2015, **6**, 5435; (*c*) F. Wang, L. Zhou, C. Zhao, R. Wang, Q. Fei, S. Luo, Z. Guo, H. Tian and W.-H. Zhu, *Chem. Sci.*, 2015, **6**, 2584.